Effect of adaptive coupling on enhancement of cerebellar learning

By Hoang Huu Thien

A thesis submitted to
School of Information Science,
Japan Advanced Institute of Science and Technology,
in partial fulfillment of the requirements
for the degree of
Master of Information Science
Graduate Program in Information Science

Written under the direction of
Associate Professor Masashi Unoki

September, 2011

Effect of adaptive coupling on enhancement of cerebellar learning

By Hoang Huu Thien (0910214)

A thesis submitted to
School of Information Science,
Japan Advanced Institute of Science and Technology,
in partial fulfillment of the requirements
for the degree of
Master of Information Science
Graduate Program in Information Science

Written under the direction of
Associate Professor Masashi Unoki

and approved by
Associate Professor Masashi Unoki
Professor Jianwu Dang
Associate Professor Isao Tokuda

August, 2011 (Submitted)

Contents

List of Figures

List of Tables

Chapter 1

Introduction

1.1 Overview

The cerebellum is a small region of the brain that plays a central role in motor control [1]. It integrates inputs from sensory systems and other parts of the brain to fine tune motor activities. The cerebellum enables animals and humans to move objects accurately and smoothly even at a high speed and without visual feedback as results of learning [2]. Several decades of both anatomical and theoretical works have resulted in deep knowledge about models of the cerebellum [3], [4] which derive from early studies formulated by David Marr and James Albus [5], [6]. It is widely accepted that the cerebellar learning takes place at Purkinje cells since they are only outputs of cerebellar cortex. Purkinje cells (PC) receive two types of input: about 200,000 parallel fibers from Granule cells and a sole but powerful climbing fiber from inferior olive (IO). Climbing fiber will cause long-term depression that reduces the efficacy of Purkinje cell synapses in hours or even longer, and it has been shown to be very important for cerebellar learning.

Although the anatomy and physiology of main elements involved in cerebellar learning, such as Purkinje cell, has been clearly described, there are some unclear aspects in cerebellar learning has more to be explored. One of these problems is the error transmission from Inferior olive. It is clear that inferior olive transmits error signals to correct motor commands produced by Purkinje cells, but how the inferior olive transmits these signals with high temporal resolution despite its low firing rate?

To overcome this problem, Schweighofer *et al.* proposed a hypothesis of chaotic resonance in which IO cells are coupled via gap junctions to induce irregular and anti-phase spiking activities of IO neurons [7]. It suggested that an intermediate coupling between IO cells may enhance error transmission from IO, thus as to enhance cerebellar learning. Recently, Tokuda *et al.* proposed a computational model of inferior olive neurons implemented chaotic resonance hypothesis to accelerate motor learning for multi-joint arm control [8]. However, these both studies have no consideration on how to realize such a coupling mechanism in real IOs. The difficulties of resolution for this issue are because a huge amount of neurons and complicated organization on several anatomical levels are observed in the cerebellum [9]. Moreover, recent studies has been shown that

there are more than one plasticity mode involved in the cerebellar learning [1], [9]. These modes make tremendous flexibility of the cerebello-olivary neuronal networks. Therefore, modeling cerebellar learning is really a big challenge for researchers in neuroscience.

As the first step towards resolving the above challenge, the thesis implements a novel idea firstly hypothesized by Kawato *et al.* [10]. This hypothesis integrates previous hypotheses with both experimental and anatomical evidences in order to optimally control the coupling in two phases of learning: in the early stage of learning, synchronously firing activities of IO cells and its innervated PCs could correct motor commands quickly for fast learning; while in the late stage of learning, weak or no synchronization of IOs could realize sophisticated learning in the cerebellum. If this approach catches some enhancements, we could find a promising framework for extended models of cerebellar learning.

1.2 Thesis goal

As a further study of [8], this research concentrates on investigating effects of adaptive couplings on cerebellar learning. Then, the thesis proposes a computational model that physiologically controls the coupling between IO neurons based on hypothesis of two-stage learning. The main purpose of the thesis is to show advantages of adaptive coupling on cerebellar learning towards constructing a framework of microzone, which consist of Purkinje cell-cerebellar nucleus-Inferior olive, for modeling cerebellar networks.

1.3 Outline of thesis

Coming after this introduction, the thesis is organized by other five chapters as follows:

- In **Chapter 2**, backgrounds of cerebellar learning, especially the role of error transmission from inferior olive in learning, are described. This thesis then emphasizes what are problems of controlling coupling between IO neurons and also suggests a plausible approach for this challenge.

- The hypothesis of two-stage learning suggested by Kawato *et al.* is demonstrated in **Chapter 3**. This hypothesis provides a novel solution for modeling cerebellar learning. In this chapter, the triangle closed-loop of Purkinje cell-cerebellar nucleus-inferior olive is also proposed to optimally control the coupling in two stages of learning.

- Next, **Chapter 4** demonstrates the feedback error learning in multi-joint arm control, and importantly, the adaptive patterns of controlling coupling between IO cells. The evaluation methods such as mutual information and synchronization index are also mentioned in this chapter.

- Purposes and procedure of thesis experiments are described in **Chapter 5**. Results of learning, which are significantly enhanced by adaptive patterns, are also discussed

in this chapter. Advantages of mutual information and synchronization index in two stages of learning show novelty and correctness of the proposed hypothesis.

- Finally, the thesis describes summary, contributions as well as future works of our research in **Chapter 6**.

Chapter 2

Backgrounds

2.1 The cerebellar learning

The cerebellum is a small region of the brain that plays an important role in motor control. It makes up about 10 percent of brain's volume but contains more than 50 percent of the neurons.

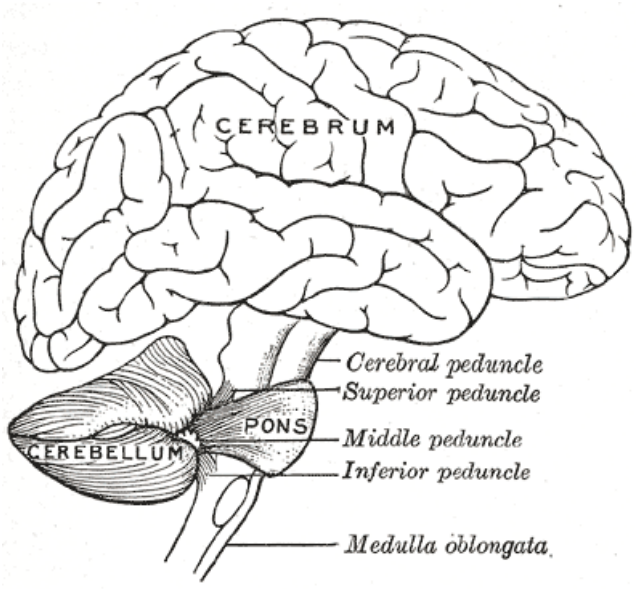

Figure 2.1: The cerebellum (*source*: Wikipedia)

Although the cerebellum is involved in some cognitive functions such as attention and language but its primary function is to make precise, accurate motor commands in movement control [1]. It detects the motor error by comparing the desired trajectory and the actual trajectory, and through its projections to upper motor control parts in cerebral cortex to reduce error as the learning proceeds. These corrections can be made both during the course of the movement and as a form of motor learning.

In general, there are two sources of information involved in cerebellar learning. The first one is the pathway of mossy fiber - granule cell - parallel fiber - Purkinje cell which carries many kinds of sensory inputs from cerebral cortex. The second source comes from Inferior olive which act as a "teacher" helping to correct motor commands produced by Purkinje cells. Therefore, the cerebellar learning acts as a closed loop of supervised learning.

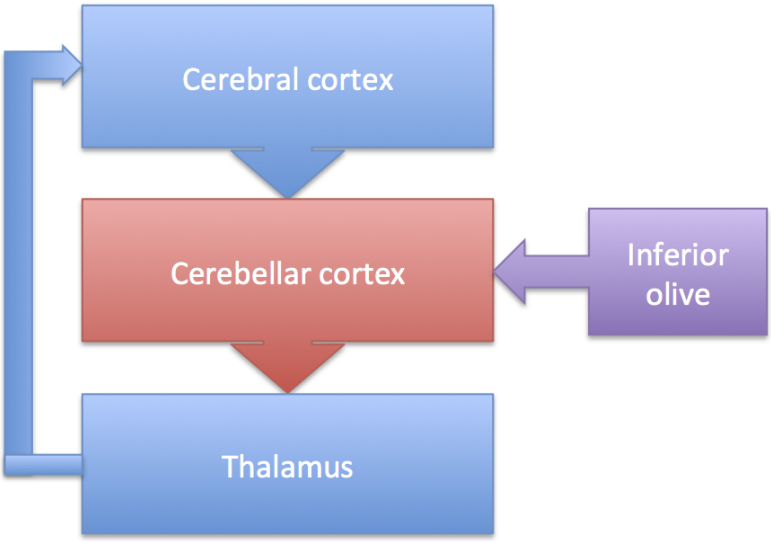

Figure 2.2: The cerebellar learning loop

Regardless of the complex structure of the cerebellar cortex, Purkinje cells form the heart of the cerebellar learning among other cellular components of the cerebellar cortex since they are its only output [1]. PCs receive two types of excitatory inputs: about 200,000 parallel fibers (PF) arising from Granule cells (GC), which have been shown transfer sensory inputs and a sole but powerful climbing fiber (CB) originating from inferior olive. Here, the climbing fiber transmits error signals from the IO. When PC is conjointly activated by the two inputs, the climbing fiber causes the long term depression (LTD) which decreases the influence of the parallel fiber-PC synapse transmission lasting hours or longer, and according to recent findings, it also impairs climbing fiber synapse transmission [2]. LTD occurs in many areas of the nervous system and it has been hypothesized to be important for motor learning because if the Purkinje cells continuously increase in strength, its synapses could reach the highest level of efficiency and thus inhibit the encoding of new information [1]. Most theories that assign learning to the circuitry of the cerebellum are derived from classical ideas of David Marr [5] and James Albus [6]. However, the challenges of modeling the cerebellum come from tremendous flexibility of cerebello-olivary neuronal networks. For example, long-term potentiation (LTP), an opposite process of LTD, also occurs at parallel fiber-Purkinje cell synapses as another synaptic plasticity. Hence, there are at least two competitive forms of long-term plasticity involved in cerebellar learning.

Once the signals are finally integrated in the PC, the cerebellar cortex output is conveyed by PC axons to cerebellar nucleus (CN) neurons which then forward motor com-

mands to the thalamus from the dentate nucleus, and then to the motor cortex for movement control [2].

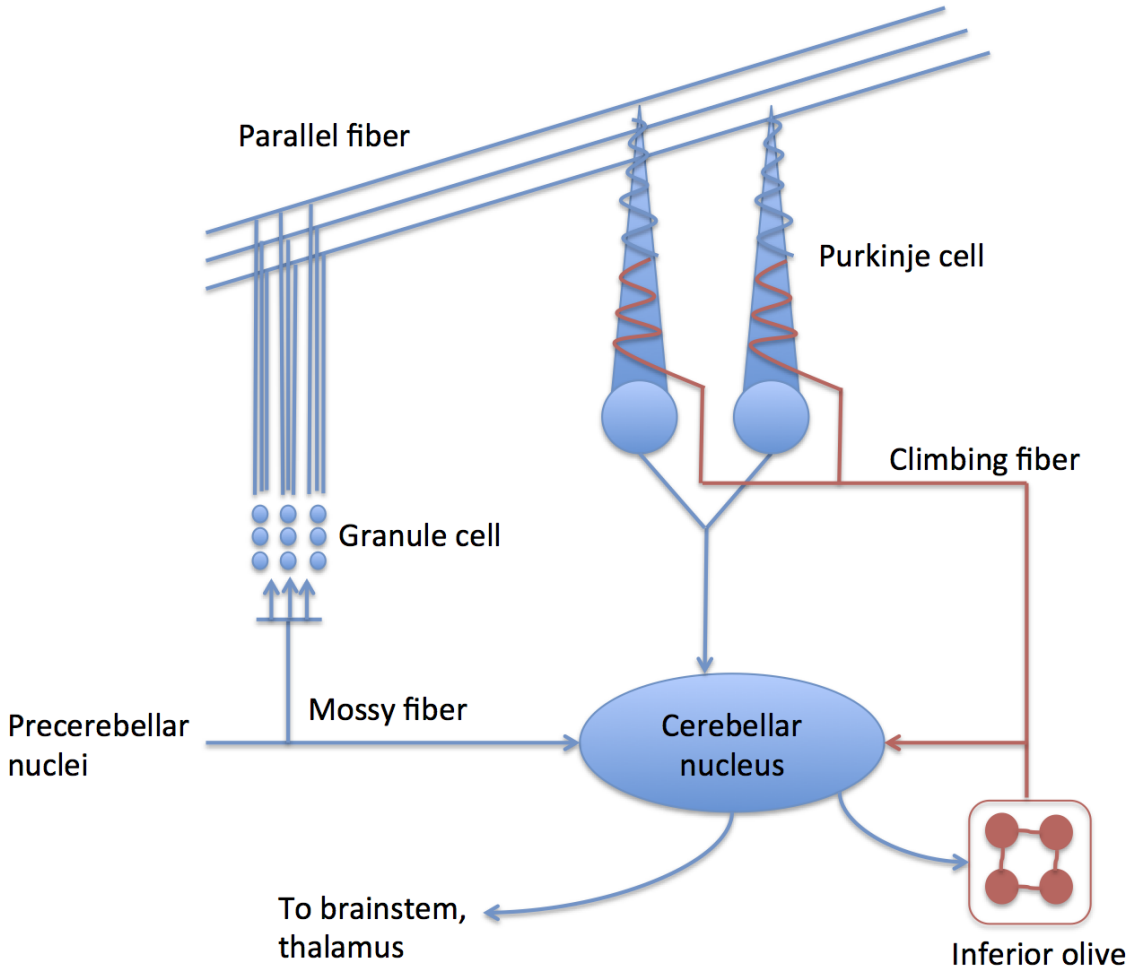

Figure 2.3: Cerebellar learning at Purkinje cell synapses

2.2 Feedback error learning

Although structures of various regions of the cerebellum are somehow different, the computational model for movement control in the brain is uniformed as Figure **??**. First, movement is planned at visual coordinates rather than muscle level. Next, the desired trajectory must be transformed into body coordinates. Finally, the motor cortex produces motor command (muscle torque) for actual movement. Consequently, the central nervous system must presents these steps for motor control.

Among computational models of the cerebellum in movement control, the feedback error learning model proposed by Kawato *et al.* [4] was ideally coherent with different regions in the cerebellum. In this model, the cerebellum acquires an inverse model of

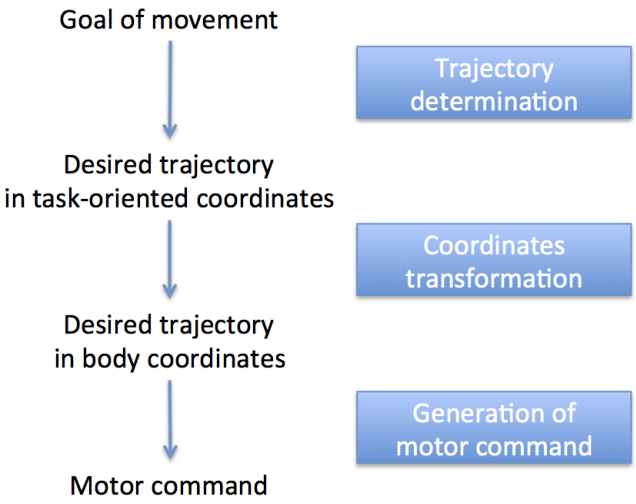

Figure 2.4: A computational model for control of movement

the controlled object. That means the input and output of the inverse model correspond to the output and input of the controlled object, respectively. Moreover, there exists a teaching signal for correcting motor commands. However, in the realistic approach, the teacher can not access to motor commands but only the desired high-level trajectory. Thus, the feedback controller must convert such trajectory errors to motor errors in order to train the inverse model. Hence, the climbing fiber is assumed to convey motor errors rather than trajectory errors.

For exploring this approach further, a computational model of the cerebellum based on feedback error learning has been proposed as follows [4]. The total torque $\tau(t)$ fed into controlled object is the sum of the feedback torque $\tau_c(t)$ and the feedforward torque $\tau_n(t)$ calculated by feedforward controller which is an inverse model of the controlled object.

$$\tau(t) = \tau_n(t) + \tau_c(t) \tag{2.1}$$

The inverse model receives the desired trajectory θ_d, then the feedforward torque $\tau_n(t)$ is computed from the desired trajectory θ_d and the synaptic weights w:

$$\tau_n = \Phi\left(\mathrm{d}^2\theta_d/\mathrm{d}t^2, \mathrm{d}\theta_d/\mathrm{d}t, \theta_d, w\right) \tag{2.2}$$

Here, the shape of the function Φ depends on what kind of neural network actually composes the feedforward controller.

The PDA feedback controller could be utilized to calculate feedback torque from desired trajectory θ_d and actual trajectory θ by:

$$\tau_c = K_P(\theta_d - \theta) + K_D(\dot{\theta}_d - \dot{\theta}) + K_A(\ddot{\theta}_d - \ddot{\theta}) \tag{2.3}$$

As the learning proceeds, the feedback motor command tends towards zero by the synaptic modification rule:

$$\mathrm{d}w/\mathrm{d}t = \left(\frac{\partial \tau_n}{\partial w}\right)^T \tau_c \tag{2.4}$$

Because the feedback motor command is used as the error signal, this model is called feedback error learning. Moreover, the long term depression in Purkinje cells may be the plasticity mechanism in feedback error learning. In this case, the output of a Purkinje cell y is the linear weighted summation of parallel fiber input x:

$$y = \sum_n w_i x_i \tag{2.5}$$

where w_i is the synaptic weight of the ith parallel fiber-Purkinje cell synapse. Then, the synaptic modification rule based on LTD is

$$\mathrm{d}w_i/\mathrm{d}t = -x_i\,(F - F_{\mathrm{spont}}) \tag{2.6}$$

where F is the firing rate of the climbing fiber input and F_{spont} is its spontaneous level. This rule strictly agrees with the synaptic plasticity in Purkinje cells: if F is higher than F_{spont}, w_i decreases. This means the efficacy of the parallel fibers decreases in long term depression. By contrast, if F is lower than F_{spont}, w_i increases. This corresponds to the long term potentiation which occurs when only parallel fibers are excited and the climbing fibers are silent.

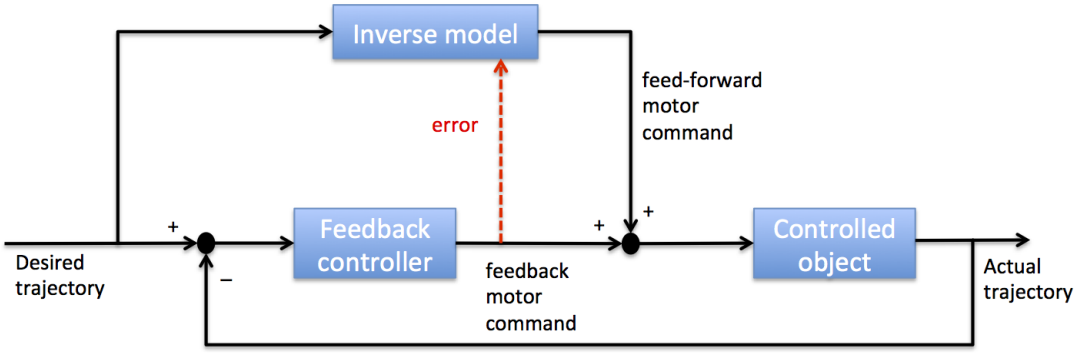

Figure 2.5: Feedback error learning model

2.3 Error transmission from Inferior olive

Purkinje cells receive input from climbing fibers that transmit error signal from IO. Although the IO lies in other parts of brain, its output goes entirely to the cerebellum. A climbing fiber also gives collaterals to the CN before entering the cerebellar cortex, where it splits into about 10 terminal branches, each of which innervates a single Purkinje cell [2]. In contrast to the 200,000 inputs from parallel fibers which cause simple spike of PC, each Purkinje cell receives input from exactly one climbing fiber; but this single fiber is so powerful that a single action potential from a climbing fiber induces a burst of several action potentials in a target Purkinje cell, a complex spike. Therefore, it has been widely accepted that climbing fiber plays an important role in cerebellar learning.

Moreover, the IO must transmit error signals with high temporal resolution at a low firing rate so that complex spikes encoding error signals do not interfere with simple spikes carrying motor commands. That requirement must be met to realize efficient motor control of the cerebellum.

Figure **??** illustrates error transmission scheme from Inferior olive. First, IO cells receive common inputs at high resolution. Like other types of neurons, when IO cells are stimulated enough by their inputs, they will fire at different timings. Although the error signal is not explicitly reconstructed, LTD can restore high-frequency information of the error signal for PCs. If IO cells fire regularly and synchronously, they do not respond to the remaining part of the input and thus IO cells exhibit a sharp peak shape waveform. By contrast, if IO firing is irregular and desynchronized, the output signal is more similar to the input waveform.

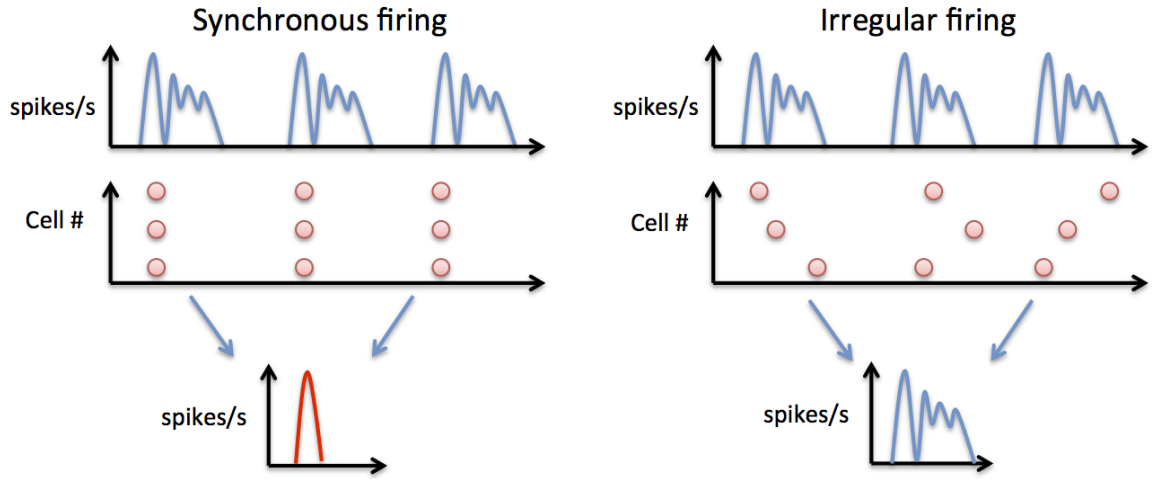

Figure 2.6: Error transmission from Inferior olive

However, how to realize such firing activities in coupled IO neurons? For resolution of this problem, Schweighofer *et al.* proposed a chaotic resonance hypothesis in which IO neurons are coupled via gap junctions to induce irregular or even chaotic spike firing [7]. There are two competing factors influencing synchronization in the IO activity: common inputs make IO neurons synchronously fire, but the coupling between these cells desynchronizes its firing activity. Therefore, a moderate coupling between IO cells could increase information transmission in IO.

2.4 Challenges of controlling coupling between inferior olive neurons

Recently, Tokuda *et al.* used a simplified model for the electrically coupled IO neurons in order to accelerate motor learning in multi-joint arm simulation [8]. They found that there exists an intermediate strength of coupling that maximizes the complexity of chaotic

firings and simultaneously optimizes the information transmission. They also stated that desynchronization of the neural firings is essential for realizing efficient information transfer. However, in this study, the coupling strength is always fixed and no consideration has been made on how to realize such a coupling mechanism in real IOs.

These challenges motivate us to find a realistic scheme for controlling coupling in real IOs. Fortunately, a novel hypothesis of two-phase learning is currently proposed by Kawato *et al.* [10]. The authors hypothesize that in the early stage of learning, the strong and synchronously firing of IO cells and its innervated PCs is useful while weak or no synchronization might be beneficial in the late phase of learning. They also suggested the triangle circuit of PC-CN-IO for physiologically controlling coupling between IO cells in cerebellar learning. Hence, our purposes are to test that hypothesis and then construct a framework for coupling mechanism of real IOs in this thesis. **Chapter 3** describes in details about hypothesis of two-phase learning. Then, our main effort contribution of methods and experimental results are mentioned in **Chapter 4** and **Chapter 5**, respectively.

Chapter 3

The proposed two stages of cerebellar learning

3.1 Hypothesis of two-phase-learning

Although the cerebello-olivary network is anatomically organized so complicated at cellular levels, it is widely accepted that the main function of IO is to carry error signals via climbing fibers to correct motor commands produced by PC. But, climbing fibers should have high temporal resolution despite its low firing rate (just few Hz) so that complex spikes encoding error signal do not interfere simple spikes carrying motor plans. To tackle this issue, Schweighofer *et al.* showed that coupled IO neurons induced irregular or even chaotic firing activities to enhance error transmission from IO [7]. Moreover, recent experimental data anatomically support the fact that only poorer error information can be transmitted when IO cells are strongly coupled and oscillated in phase. However, possible functions of PC-CN-IO closed circuit for controlling IO coupling are quite unclear, especially the inhibitory synapses on the dendrites of IO cells close to their gap junctions within glomeruli.

For investigating inhibitory effect of CN, Kawato *et al.* hypothesized that the triangle circuit and the inhibitory synapses from CN to IO are the neural mechanisms to optimally control the coupling between IO cells in the two-stage learning as follows [10]. In the early stage of learning, because the actual trajectories are quite different from the desired trajectories, motor commands must be highly modulated, since error signals are large. If many PCs fire synchronously and change their firings by almost the same error signals, the learning should be very fast from the early stage due to huge changes of motor commands. Thus both mossy fibers and climbing fibers are strongly active. Hence, both PC and IO cells fire strenuously as the CN cell are depressed. The inhibitory synapses are inactive within IO glomeruli, and the IO cells are strongly coupled. As a consequence, IO cells and the innervated PCs are synchronously excited.

By contrast, in the late stage of learning, since the actual trajectories are precise and close to those desired, both mossy fiber and climbing fiber inputs are weak. Hence, both PC and IO cells rarely fire and the CN cell are strongly excited due to disinhibiting

from PC. Because inhibitory synapses are active within the IO glomeruli, the IO cells are only weakly coupled. Therefore, IO cells and innervated PCs are asynchronously fired. Importantly, those firing might be chaotic as suggested from [7].

Figure 3.1 illustrates possible functions of the PC-CN-IO circuit for controlling the coupling between IO cells in two stages of learning. Red neurons are excited, and blue neurons are depressed. PC projects its outputs to CN as inhibitory signals, and CN also sends GABAergic neurotransmitters to control electrical coupling between IO cells. Neuronal activities of PC-CN-IO in two stages of learning are shown in the right raster plot. The change of error signals and transmitted information of IO neurons during the learning process is also schematically described in lower parts of Figure 3.1.

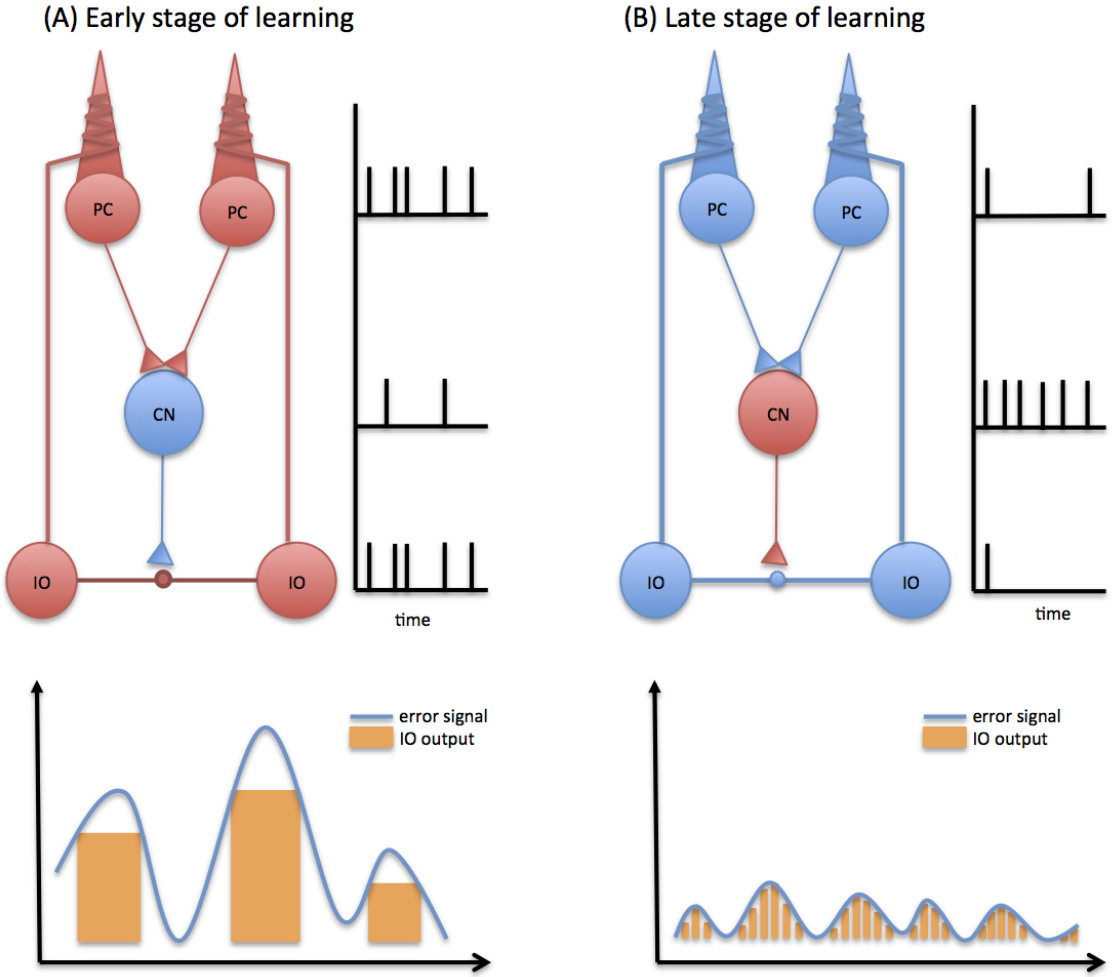

Figure 3.1: Schematic diagram illustrating possible functions of the PC-CN-IO closed circuit in the two-stage learning.

As a summary, in the early learning stage, strong synchronization is useful for modulating motor commands while weak or no synchronization might be advantageous in the late learning stage.

3.2 Purkinje cell-cerebellar nucleus-inferior olive circuit for controlling adaptive coupling

Based on hypothesis of two-stage learning in cerebellum, the thesis proposes a scenario in which PC-CN-IO circuit controls electrical coupling between IO neurons. Initially, the PF-PC synapses are relatively strong (before LTD), which activate the PC. This makes the inhibitory effects from PC to CN strong and thus the CN activity is weak. Inhibited CN cells innervate the dendrites of IO cells within glomeruli very close to the gap junctions. As a consequence, the IO cells are excited and its firing rate is high, making the coupling strength of the IO strong. As the learning proceeds, CN cells are excited and the IO cells are not only inhibited but their electrical couplings become weaker and converge to a possibly optimal value.

Chapter 4

Methods

4.1 Inferior olive model

As an implementation of chaotic resonance hypothesis, Tokuda *et al.* proposed a simplified μ-model for coupled IO neurons as follows [8]:

$$\begin{aligned} \eta_1 \frac{dx_i}{dt} &= -y_i - \mu_i x_i^2 \left(x_i - \frac{3}{2} \right) + I + J_i \\ \eta_2 \frac{dy_i}{dt} &= -y_i - \mu_i x_i^2 \end{aligned} \tag{4.1}$$

where

$$J_i = \begin{cases} g(x_2 + x_N - 2x_1) & (i = 1) \\ g(x_{i+1} + x_{i-1} - 2x_i) & (i = 2, ..., N-1) \\ g(x_1 + x_{N-1} - 2x_N) & (i = N) \end{cases} \tag{4.2}$$

x_i and y_i represent the membrane potential and ion channel activity of the ith neuron (i = 1, 2, ..., N), N is the total number of the neurons, μ is a system parameter, η_1 and η_2 are time constants, g is the coupling strength of the gap junctions, and I is an external input.

An advantage of this model is its weak dependence on parameter value. Here, μ is only the parameter that control dynamics of the neurons. Moreover, proper value for μ to generate spiking dynamics is also well understood [8].

As seen in Figure 4.1, the membrane potential activity of population of neurons is equivalent to only one neuron without coupling ($g = 0$). But it becomes irregular, anti-phase oscillators within an intermediate coupling strength ($g = 0.05$). Hence, this model is easy on applying coupling mechanism for adaptive patterns by equation 4.2. The spiking activity of the kth IO neuron is defined as a membrane potential that exceeds a threshold value. This threshold value is set as $x_{th} = 0.75$ because the couplings are always fixed in [8]. However, since the coupling is adaptively changed when the learning proceeds in the thesis, a coupling table of thresholds is correspondingly scheduled adaptive.

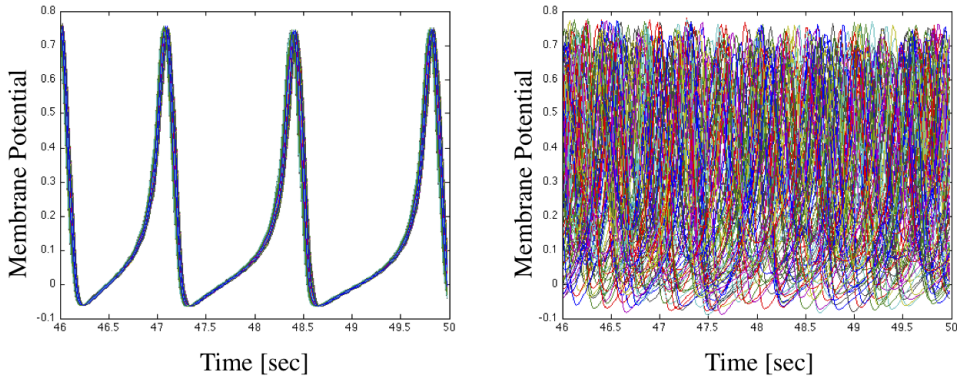

Figure 4.1: Comparison of membrane potential activity of two coupling strengths.

4.2 Feedback error learning control

Feedback error learning model is a very famous model of cerebellar learning which was proposed by Kawato *et al.* [3], [4]. In this model, the cerebellar cortex is simply composed by Granule cells and Purkinje cells and it learns as an inverse dynamics of controlled object which is a physical entity such as hands, legs, etc.

The desired trajectory is given to the inverse model which produces feedforward motor commands for movement goals. The feedback controller transforms trajectory error, which is difference between the desired and actual trajectories, into feedback motor command which is then utilized to train the inverse model. As a consequence, at the end of the learning the actual trajectory will be close to the desired trajectory.

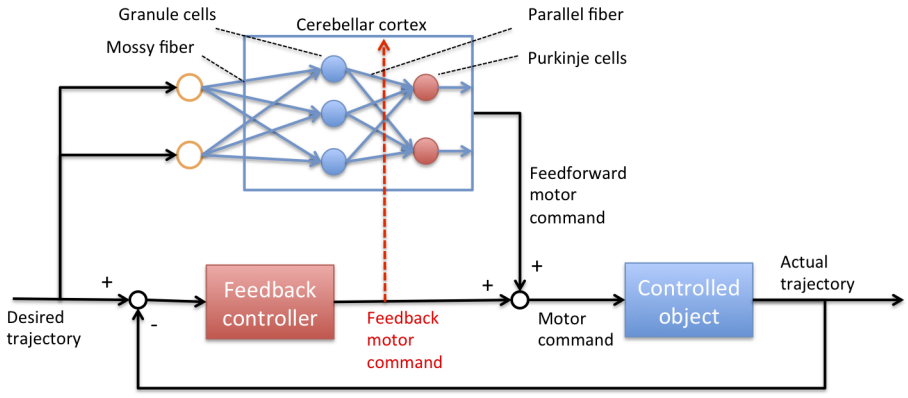

Figure 4.2: Feedback error learning control

The processing flow of this model is as follows. Granule cells receive desired state vectors $s = [\theta_e, \theta_s, \dot{\theta}_e, \dot{\theta}_s, \ddot{\theta}_e, \ddot{\theta}_s]$ then sends its output to Purkinje cells

$$GC_j = \tanh\left(\sum_i v_{ji} s_i\right) \tag{4.3}$$

$$PC_k = \sum_j w_{kj} GC_j \tag{4.4}$$

where GC_j is the jth granule cell activity, PC_k is the kth Purkinje cell activity, v represents the fixed weights from the desired state input to the granule cells, w represents the modifiable weights from the granule cells to the Purkinje cells. The only output of feedforward controller, feedforward motor command, is accumulated from PC activities. Then the vectors of motor commands are given by the sum of the feedback and feedforward motor commands, τ_{fb} and τ_{ff}, respectively:

$$\tau = \tau_{\text{ff}} + \tau_{\text{fb}} \tag{4.5}$$

A simple PD feedback controller is used for calculating feedback motor commands:

$$\tau_{\text{fb}} = K_P \cdot (\theta_d - \theta_{\text{sensed}}) + K_D \cdot \left(\dot{\theta}_d - \dot{\theta}_{\text{sensed}}\right) \tag{4.6}$$

where θ_d and θ_{sensed} are the vectors of the desired and sensed joint position.

The feedback motor commands are integrated as the learning error when the learning proceeds:

$$\text{error} = \int_{\text{t}_0}^{\text{t}_1} \tau_{\text{fb}} \cdot \text{dt} \tag{4.7}$$

t_0, t_1 are initial and final time of each learning trial, respectively, and dt is the time step.

To inject proposed inferior olive model into feedback error learning, feedback motor commands are fed into IO cells as their input signals. Then, IO cells produce output signals, which represent to climbing fiber, to adjust modifiable weights of parallel fiber-Purkinje cell synapses. The learning of feedback error model is applied by the following rule:

$$w_{kj} = w_{kj} + \alpha \cdot (IO_k - IO_{\text{mean}}) \cdot GC_j \tag{4.8}$$

where IO_k is the spiking activity of the kth IO neuron and α is a learning rate. The spiking activity IO is determined by the threshold and is mathematically defined as

$$\begin{cases} IO_k = 1, x_k \geq \text{threshold} \\ IO_k = 0, otherwise \end{cases} \tag{4.9}$$

Here, the error input to the IO cells is given by $I = I_0 + \beta \cdot \tau_{\text{fb}}$, where I_0 and β are the minimal input and the input gain, respectively. The mean firing rate IO_{mean} is averaged from firing rates of all IO cells with constant input $I = I_0$.

In order for calculating threshold value and average spiking rate IO_{mean} in case of adaptive coupling, the coupling table is constructed. Please refer to the last section of this chapter for more details about procedures of the coupling table.

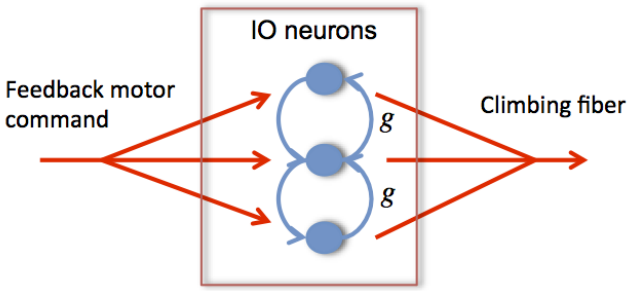

Figure 4.3: IO activities in feedback error learning.

4.3 Synchrony

In order to detect synchronized activity of the neurons, the order parameter R in Kuramoto model [17] has been utilized. The order parameter is a quantity that can be interpreted as the collective rhythm produced by the population of neurons.

$$R\exp(i\Phi) = \frac{1}{N}\sum_{j=1}^{N}\exp(i\phi_j) \tag{4.10}$$

where ϕ_j is the phase of jth neuron given by angle $\phi_j = \arctan\left(\frac{x_j(t-0.2)}{x_j(t)}\right)$. The order parameter take values between 0 and 1, where a large value close to R=*1* implies strong synchronization and a small value close to R=*0* implies desynchronization.

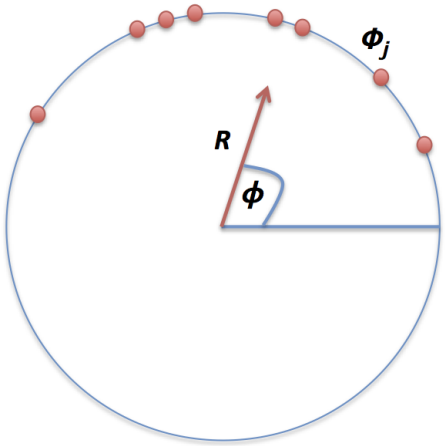

Figure 4.4: Geometric interpretation of the order parameter

4.4 Mutual information

As a basic study to evaluate the information transmission of the IO network, the simulation measures the mutual information between an input signal and the spike responses.

Input signal is the error input to the IO cells in feedback error control. The output represents a time sequence of a number of spikes generated from the population of neurons.

The mutual information were given from the formula

$$MI(X;Y) = H(X) + H(Y) - H(X,Y) \tag{4.11}$$

where X and Y are 50-bin-discretized input and output signals, $H(X)$, $H(Y)$ and $H(X,Y)$ are marginal and joint entropies of inputs and outputs, respectively.

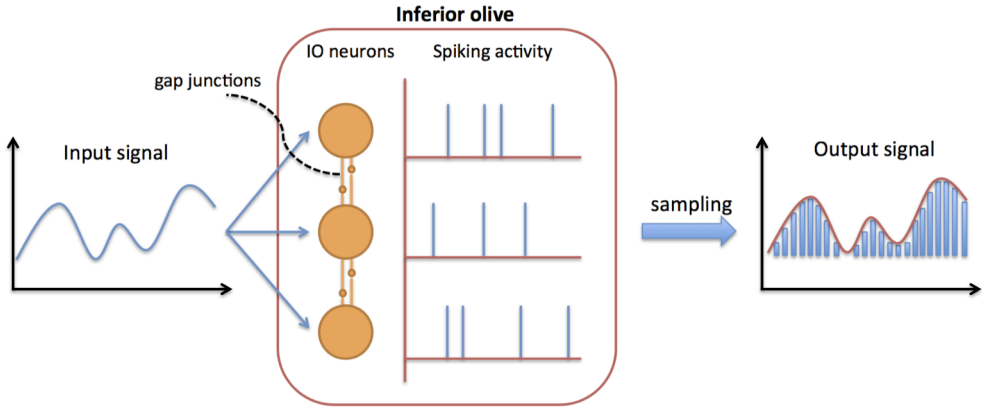

Figure 4.5: Mutual information of IO cells

Mutual information measures error transmission from IO as follows. The mutual information take values between 0 and 1, where a large value close to 1 implies effficiently transmission from IO and a small value close to 0 means IO poorly transmits the error signal.

4.5 Dependences of learning results on the fixed coupling

Using feedback error learning control, Tokuda *et al* investigated learning results of fixed coupling strengths [8]. Figure 4.6, which shows learning error, recommends that the coupling should be scheduled to decline as the learning proceeds. Initially, the strong coupling is useful for correcting motor errors since the error signals are large. But when the learning errors are small, weak coupling between IO cells could realize an efficient learning.

Figure 4.7 and Figure 4.8 shows dependences of mutual information and synchronization index on the coupling strength $g \in [0, 0.4]$, respectively. As seen in these figures, there existed an intermediate coupling around $g = 0.05$ which maximize the information transmission from IO. These results suggested that weak couplings should be utilized as desynchronization of coupled IO neurons in order to enhance error transmission from IO.

In order to evaluate enhancements of adaptive patterns, the learning results of adaptive coupling are compared with fixed coupling strength $g = 0.05$ which minimize the learning error as seen in Figure 4.6.

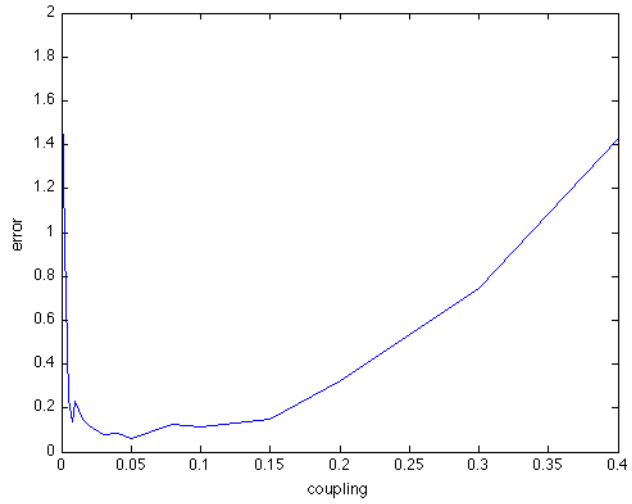

Figure 4.6: Dependence of learning error on the coupling strength.

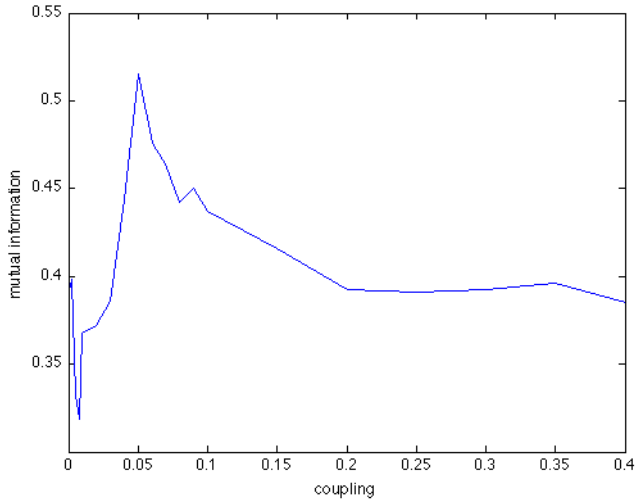

Figure 4.7: Dependence of mutual information on the coupling strength.

4.6 Adaptive coupling

In the thesis, two adaptive patterns of coupling are investigated in order to fully understand about effect of adaptive coupling on enhancement of learning. Then, a computational model of PC-CN-IO circuit is proposed to control the coupling in a realistic way. Due to adaptive changes of coupling, a coupling table of thresholds and mean firing rates is also scheduled before the learning.

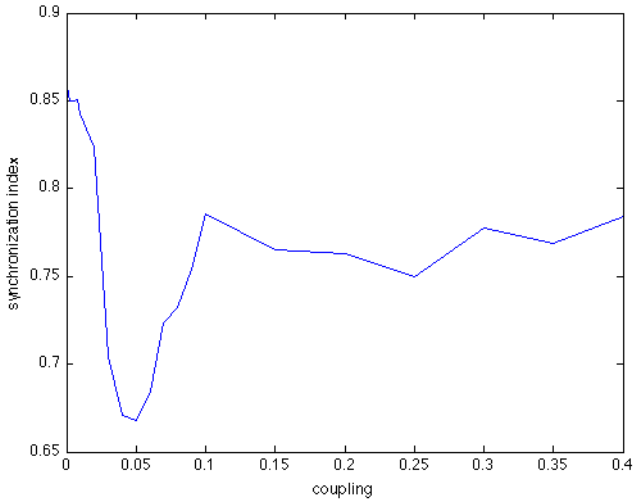

Figure 4.8: Dependence of synchronization index on the coupling strength.

4.6.1 Pattern #1: linear function of learning time

Firstly, the coupling is a linear function of learning time. As a correspondence to the hypothesis two-stage learning, in the early stage of learning the IO cells are strongly coupled, thus the coupling is strong. When the learning proceeds, the coupling decreases linearly to a very small value $g = 0.005$ and maintain this value during the late stage of learning. This simple pattern can be formulated by the adaptive pattern #1:

$$g_{\#1} = \begin{cases} a \cdot \mathrm{t} + b & (\mathrm{t} < 400[sec]) \\ 0.005 & \text{otherwise} \end{cases} \tag{4.12}$$

4.6.2 Pattern #2: linear function of error

Next, the coupling is scheduled to decline as a linear function of error. The concept of this pattern is to use error for training the learning system. In the early stage, since the error signals are large, the learning speed is expected to decrease quickly. Then in the late phase, because the error is small we can use a very small value to realize a sophisticated learning. The second pattern can be formulated by the adaptive pattern #2:

$$g_{\#2} = \begin{cases} c \cdot \mathrm{error} + d & (\mathrm{error} > 0.85) \\ 0.005 & \text{otherwise} \end{cases} \tag{4.13}$$

4.6.3 Pattern #3: Computational model of PC-CN-IO circuit

Based on hypothesis of two-stage learning, the thesis proposes a computational model to physiologically control the adaptive coupling between IO neurons. Our scenario is as follows:

- In the beginning (before LTD), the parallel fibers are not yet depressed and strong inputs come from GC, thus PC is active. Due to inhibition from PC to CN, strong PC activity makes CN less active. This makes the inhibitory synapses on the dendrites of IO cells within glomeruli weak or just a small amount of GABAergic conductance has been transmitted. As a result, IO activity gets relatively high, producing a strong coupling among IO cells.
- As the learning proceeds, LTD weakens the PC activity. The suppressed PC makes CN more excited, thus the GABAergic conductance gets large, and as a consequence the IO coupling becomes weak.

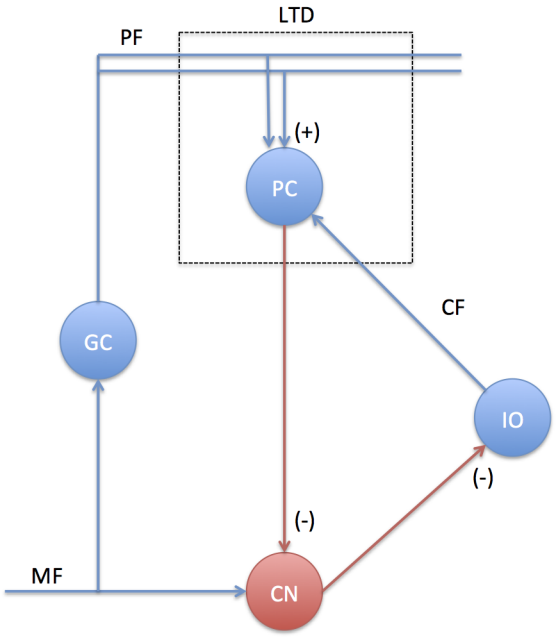

Figure 4.9: Schematic diagram of PC-CN-IO circuitry

In our study, the PC activity was measured as a summation of the parallel fibers which is preresented by synaptic weights from GC to PC. Because of the LTD, the parallel fibers become smaller and smaller taking negative values as the learning proceeds. In order to make a good correspondence to PC activity, which should take a positive value, a threshold was inserted as follows:

$$PC_{\text{activity}} = PC_{\text{threshold}} + \sum_{i,j} w_{i,j} \tag{4.14}$$

According to our scenario, GABAergic conductance from CN to IO should be inversely proportional to the PC activity. So, the GABAergic conductance was simply modeled as:

$$g_{\text{inhibitory}} = \frac{\omega}{PC_{\text{activity}}} \tag{4.15}$$

where ω is a positive constant. Finally, under simplifying assumptions, effective coupling conductance between coupled IO cells is computed from gap junction conductance g_{junction}, conductance of inhibitory synapses $g_{\text{inhibitory}}$ and from spine neck conductance g_{spine} as Onizuka' equation [14]:

$$g_{\#3} = \frac{g_{\text{junction}} \cdot g_{\text{spine}}}{g_{\text{spine}} + g_{\text{inhibitory}}} \tag{4.16}$$

Thus if the inhibitory synaptic conductance is large, the effective coupling conductance decreases because of shunting inhibitory.

In our proposed computational model of PC-CN-IO circuit, the gap junction conductance and spine neck conductance are given as $g_{\text{junction}} = 2.0$, $g_{\text{spine}} = 0.65$. Other parameters of adaptive patterns are set as $PC_{\text{threshold}} = 17$, $\omega = 27$, $a = -0.012$, $b = 0.6$, $c = 0.0372$ and $d = -1.575$.

4.6.4 Coupling table

In this study, the coupling is controlled by adaptive patterns which leads to changes of firing threshold and IO_{mean}. To overcome this issue, the simulation calculates a coupling table in which thresholds and mean firing rates are computed as following procedure:

- 1) Before learning, compute the maximum amplitude with constant input I_0 for various coupling.
- 2) Set the threshold as 80% of the maximum amplitude and compute the average firing rate of IO cells for various coupling.

Based on 1) and 2), we can construct a table for threshold and IO_{mean} for various coupling values which are set as fixed strengths from $g = 0.005$ to $g = 1.0$.

As the learning proceeds, every time the coupling value is changed, the simulation looks for the table to find the threshold and IO_{mean} associated with the coupling value close to the one used at the actual moment of learning. These values are then applied in the learning loop.

Chapter 5

Experiments and Results

5.1 Experiments

The experiment simulates multi-joint arm movement using feedback error learning control described in Appendix A. Purpose of the experiment is to show enhancements of proposed adaptive patterns in feedback error learning by comparing with fixed coupling $g = 0.05$ which has been shown to minimize the learning error in [8]. Moreover, reasonable interpretations of learning results are also very important. Hence, mutual information and synchronization index are computed to show correctness of results in two stages of learning. Synchronization index gets close to 1 when IO neurons are strongly coupled, and it gets close to 0 when IO neurons are weakly coupled. Besides, error transmission should have a good correspondence with mutual information: the higher value of mutual information is, the much better of information transfer from IO is.

5.2 Results and discussions

This section shows experimental results of simulation in 100 learning steps. In order to reduce the dependence of the neural dynamics on the random initial conditions, 50 simulations were run to compute the average quantities of learning error, mutual information and synchronization index. This requirement is one of the most important criteria of evaluating dynamics of IO neurons.

5.2.1 Coupling table

In the simulation, the coupling table is scheduled before the learning. Figure 5.1 and Figure 5.2 show thresholds and IO_{mean} of fixed coupling strengths from $g = 0.005$ to $g = 1.0$, respectively.

Since the thresholds are computed from maximum amplitudes of IO neurons, Figure 5.1 shows the decrease of thresholds depends upon the coupling strength. It is because the membrane potentials get high when IO cells strongly coupled. Moreover, the percentage

80% of maximum amplitudes is also tested to be a reasonable value for computing thresholds. Based on these thresholds, the IO_{mean} resulted as the same value in the range of $g \in [0.005, 0.9]$. This makes a fair circumstance in comparison between adaptive couplings and fixed coupling: although IO_{mean} does not change as the learning proceeds, the change of thresholds ideally control the firing rate of IO cells.

Table 5.1 list out thresholds and average spiking rate of fixed couplings in range of $g \in [0.005, 1.0]$.

Table 5.1: Coupling table

Coupling (g)	Threshold	Average spiking rate (spikes/sec)
0.005	0.7788	0.0310
0.01	0.7798	0.0310
0.02	0.7770	0.0310
0.03	0.7833	0.0310
0.04	0.7837	0.0310
0.05	0.7834	0.0309
0.06	0.7798	0.0309
0.07	0.7888	0.0310
0.08	0.7875	0.0309
0.09	0.7900	0.0310
0.1	0.7879	0.0310
0.2	0.7946	0.0310
0.3	0.7961	0.0309
0.4	0.7964	0.0309
0.5	0.7973	0.0310
0.6	0.7977	0.0310
0.7	0.7961	0.0310
0.8	0.7974	0.0310
0.9	0.7951	0.0310
1.0	0.7927	0.0320

5.2.2 Learning error

Figure 5.3 shows three adaptive patterns of coupling compared with fixed coupling $g = 0.05$. The coupling strength of all adaptive couplings are initially set around $g = 0.6$. This initial coupling is examined to maximize the learning speed in the early stage of learning. By contrast, the final coupling $g = 0.005$ provides sophisticated learning since the errors are small. These adaptive couplings strictly agree with hypothesis of two-phase learning. As a consequence, the learning error of all adaptive patterns are significant enhanced not only in the early stage of learning with quickly decay of error, but also the final error (Figure 5.4).

Importantly, as seen in Figure 5.3, coupling functions of three patterns are same together. This is because the second and the third patterns are designed to map with the

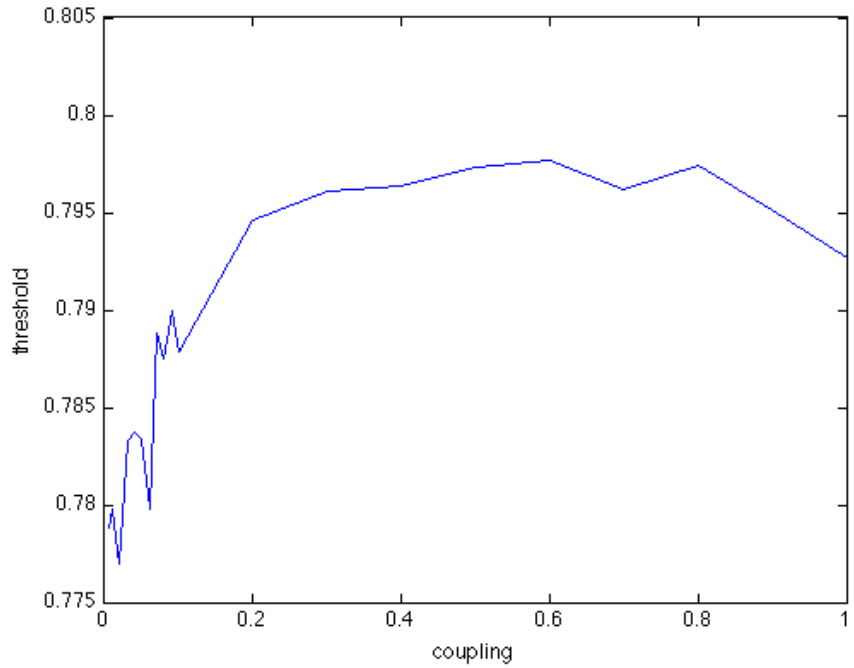

Figure 5.1: Firing thresholds of coupling table.

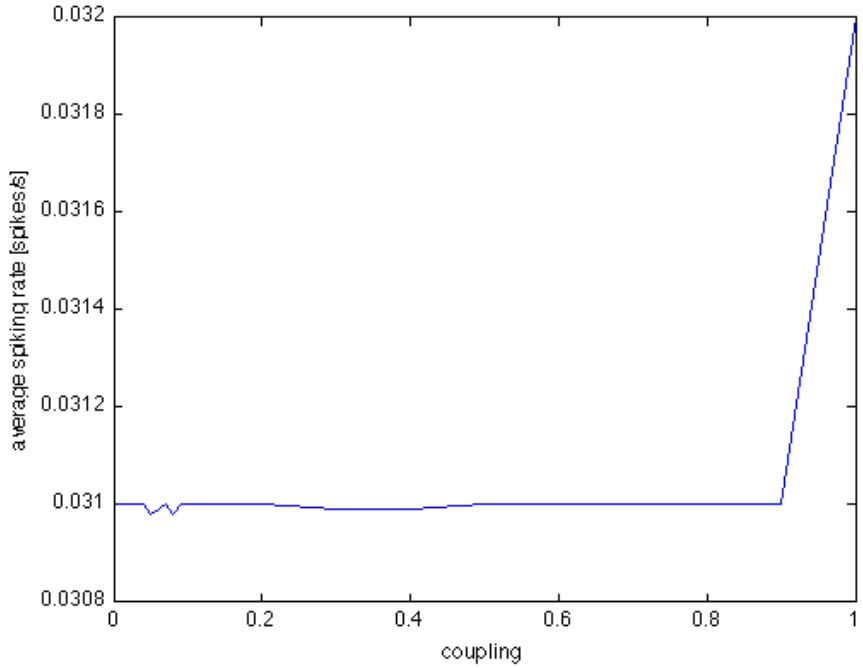

Figure 5.2: Means of IO firing of coupling table.

first pattern as the learning proceeds. The purpose of these adaptive couplings is not to show advantages of different patterns, but the coupling could be controlled by different patterns for enhanced learning. These experiments are very important in order to realize deeply understandings about the cerebellar learning.

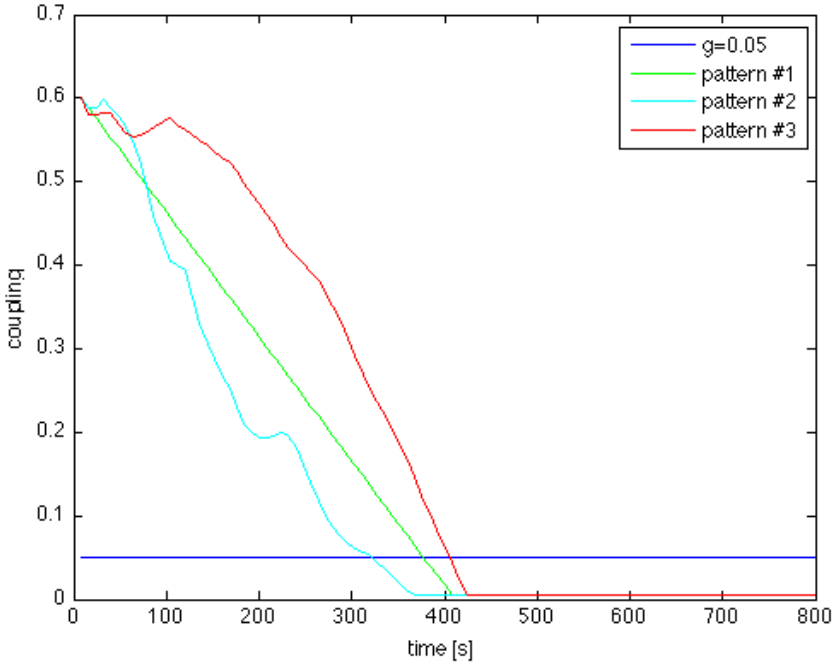

Figure 5.3: Coupling functions

In order to check whether adaptive coupling could realize efficient learning compared with fixed coupling, the thesis do a hypothesis testing to compute significant difference of the final errors between adaptive coupling pattern #1 and fixed coupling $g = 0.05$ at the 0.05 significance level. Statistical data of the experiment is as Table 5.2.

Table 5.2: Statistical data of the hypothesis testing

Statistical data	Fixed coupling $g = 0.05$	Adaptive coupling #1
Mean of final errors	$X_1 = 0.8023$	$X_2 = 0.7724$
Standard deviation	$s_1 = 0.0032$	$s_2 = 0.0037$
Number of samples	$n_1 = 50$	$n_2 = 50$

The hypotheses are stated as:

- *null hypothesis* H_0: $X_1 - X_2 = 0$
- *alternative hypothesis* H_1: $X_1 > X_2$

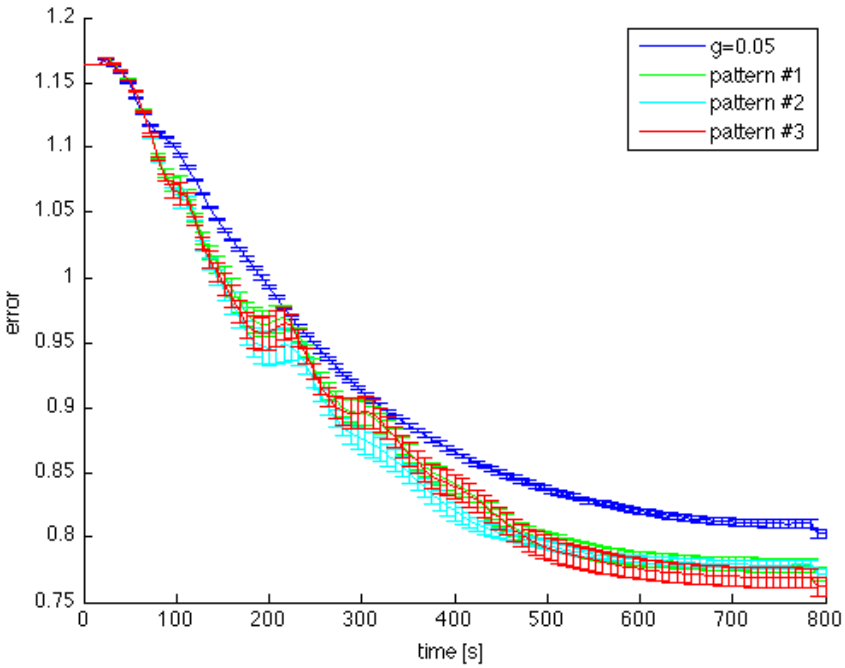

Figure 5.4: Learning error

The *t-value* of this test is given by:

$$t = \frac{(X_1 - X_2)}{\sqrt{\frac{s_1^2}{n_1} + \frac{s_2^2}{n_2}}} = 43.22 \tag{5.1}$$

The degrees of freedom *df* of the test is computed by:

$$df = \frac{\left(\frac{s_1^2}{n_1} + \frac{s_2^2}{n_2}\right)^2}{\frac{\left(\frac{s_1^2}{n_1}\right)^2}{n_1 - 1} + \frac{\left(\frac{s_2^2}{n_2}\right)^2}{n_2 - 1}} = 96.01 \tag{5.2}$$

Because the p value of this test is very small and close to 0 (p=2.7366e-64), thus the test rejects the null hypothesis at the significance level 0.05. That means there is a sufficient evidence to make a conclusion about significant improvement of the final error of the adaptive pattern compared with fixed coupling $g = 0.05$.

5.2.3 Error transmission

The results of mutual information in Figure 5.5 also support our hypothesis of two-stage learning. In the beginning of learning, since the error signals are large, the synchronized IO cells concentrate to modulate the motor commands that are much more than level of trajectory errors. Thus the learning is quite quick although the mutual information

of adaptive patterns are smaller than the fixed coupling $g = 0.05$ in the early stage of learning. But the adaptive patterns maintain a very small value $g = 0.005$ in the late phase of learning. Hence, the mutual information of adaptive couplings gets higher than the fixed coupling to realize an efficient learning. As a consequence, the learning error continues to decreases further and the final error of adaptive patterns gets small.

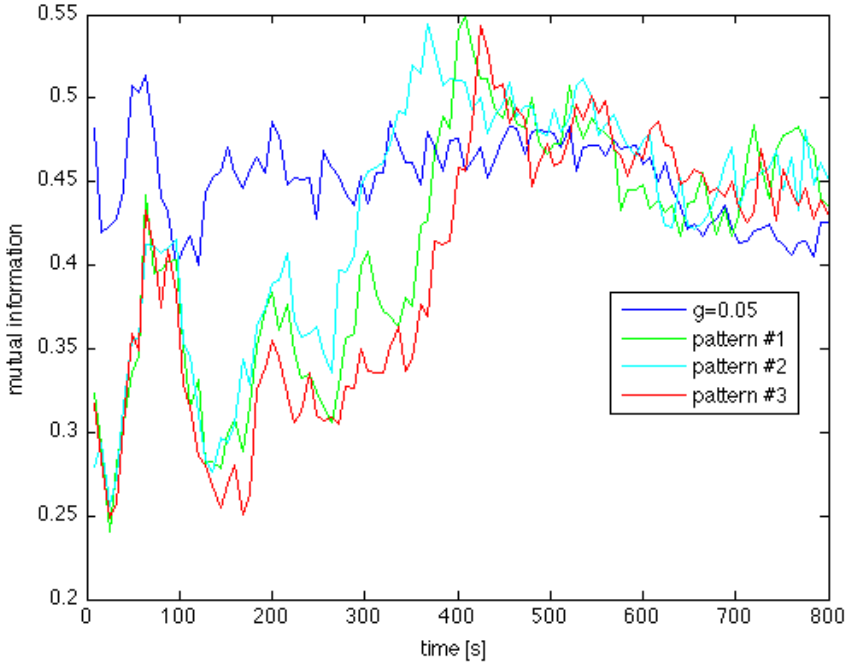

Figure 5.5: Mutual information

5.2.4 Synchronization index

Initial learning procedure is comparable between the fixed coupling and the adaptive coupling patterns. In the final stage of learning, adaptive couplings show lower error than the fixed coupling. As seen in Figure 5.6, the adaptive couplings initially give rise to synchronous neuronal activities for quick learning. Then, as the learning proceeds, the synchronization indices become smaller to make the learning more efficient as final sophisticated learning. In the contrary, the synchronization index is flat for the fixed coupling. This might be one of the reasons why the adaptive couplings provide better learning than the fixed coupling and strictly agrees with our scenario.

5.2.5 Discussions

Learning results of adaptive patterns show advantages of adaptive coupling on enhancement of cerebellar learning. With respect to synchronization, there are two competing

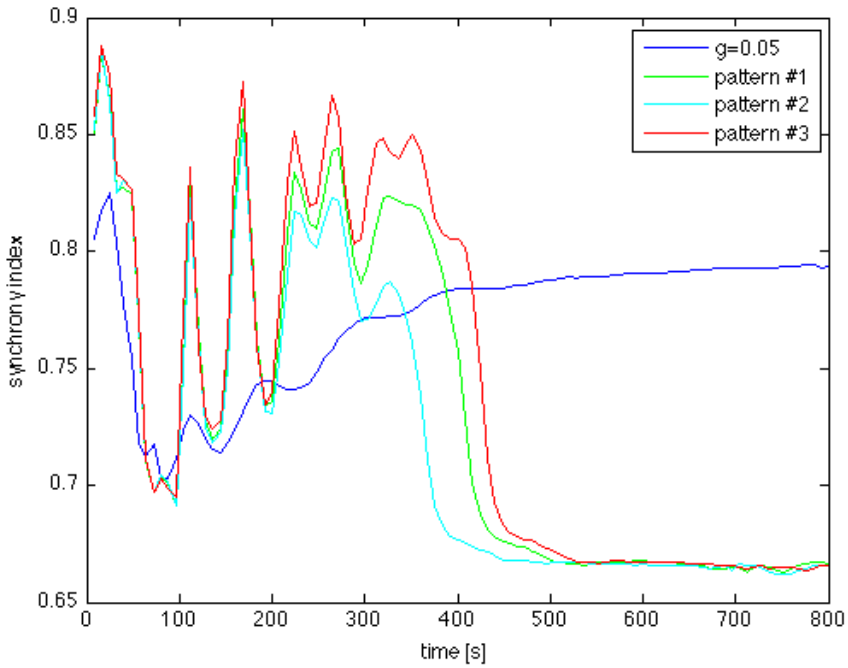

Figure 5.6: Synchronization index

factors: (i) common input to induce synchrony among the neurons, and (ii) intermediate coupling to destroy synchrony among the neurons.

By applying three adaptive patterns, the cerebellar learning successfully integrated two competing factors in a plausible circumstance. In the initial stage of learning, the input signal is large because the error is large. This induces a strong synchrony among the neurons. To destroy the synchrony, a strong or intermediate coupling is utilized. As the learning proceeds to the final stage, the input signal becomes small, because the error is decreased. This weakens the effect of inducing the neural synchronization. Therefore, it does not need a too strong coupling for destroying synchronization. That is why a considered $g = 0.005$ is chosen for the final learning.

Finally, improved learning results of the third adaptive pattern provide a promising scheme for control the firing activities of IO cells for enhancement of cerebellar learning.

Chapter 6

Conclusion

6.1 Summary

Concerning firing activity of neurons in cerebellar learning, the thesis implemented a hypothesis of two-stage learning, in which PC-CN-IO circuit is proposed to optimally control the coupling between IO neurons. In the early stage of learning, the IO cells and innervated PCs are strongly and synchronously fire in order to correct the error signals quickly. Then in the late phase of learning, inhibitory synapses from excited CN make IO cells are only weakly coupled for sophisticated learning.

To test above hypothesis, the thesis implemented three adaptive patterns of couplings:

- *Pattern #1:* the coupling is a linear function of learning time.
- *Pattern #2:* the coupling is scheduled to decline as a linear function of error.
- *Pattern #3:* a computational model of PC-CN-IO circuit was proposed to optimally control firing activities of coupled IO cells.

Improved results from experiments of adaptive patterns compared with the intermediate coupling $g = 0.05$ are suited with observations of mutual information which represents error transmission from IO and synchronization index which represents synchronized firing activities of IO cells. Not only the final error but also the quick decay of error in beginning of learning can be realized. Moreover, mutual information and synchronization index also supported interpretations in two stages of learning. They recommended that hypothesis of two-stage learning is ideally a plausible approach for controlling firing activities of IO cells in long lasting learning.

6.2 Contributions

The most important contribution of the thesis is to show effects of adaptive coupling on enhancement of cerebellar learning by implement hypothesis of two-stage learning. A simple computational model of PC-CN-IO circuit is also proposed to optimally control

the adaptive coupling between IO cells. The thesis also provides a solid framework of cerebellar learning for resolution of more generalization problems.

6.3 Future works

In the thesis, the learning results of adaptive patterns are significant enhanced compared with fixed coupling. However, optimized pattern of adaptive coupling might increase performance of learning results. Hence, we will concentrate on optimizing adaptive pattern by artificially changing the coupling between IO neurons.

Besides, our proposed model of Purkinje cell-cerebellar nucleus-inferior olive is not completely a realistic model of the cerebellum, since CN activity is utilized to control the coupling of IO neurons via the PC-CN-IO pathway. As a future work of this thesis, we will propose a computational model of PC-CN-IO as a physiological framework for controlling firing activities of IO cells for enhanced cerebellar learning.

Appendix A

Two degree-of-freedom human arms movement

In the simulation, the feedback motor learning controller controls a two degree-of-freedom human arm as in [8]. The arm which is composed by the shoulder and the elbow tends to reach four targets forming a square of 20×20 cm on a horizontal plane with a movement time of 2s. The center location of the square is [0,0.4] m, where the shoulder is located at [0,0].

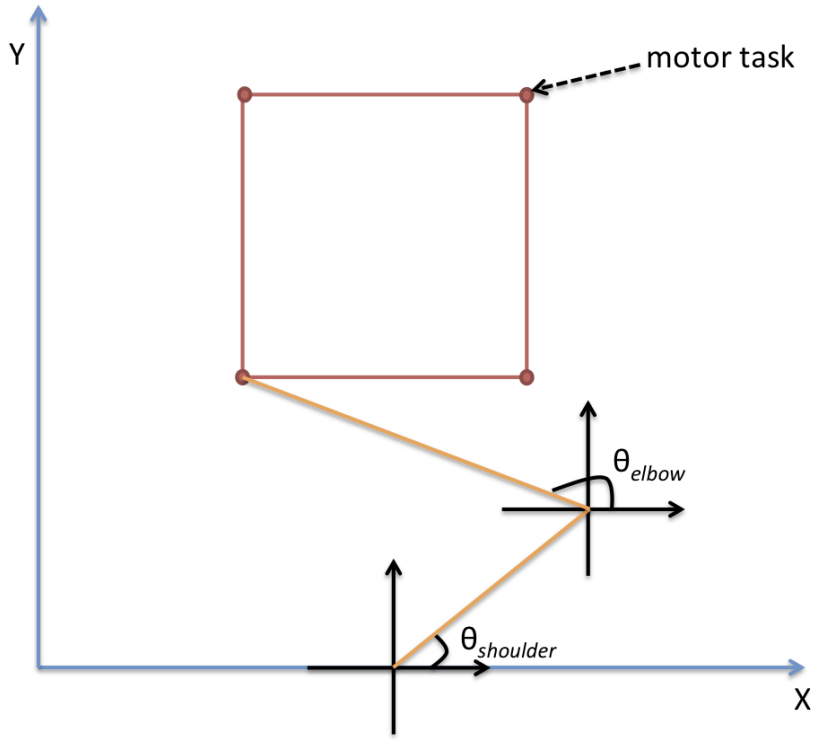

Figure A.1: Two degree-of-freedom human arms movement

The arm dynamics is given by

$$M(\theta)\ddot{\theta} + C(\dot{\theta}, \theta)\dot{\theta} = \tau \tag{A.1}$$

where θ is the vector of the arm joint angles and τ is the motor command. The inertial and Coriolis matrices M and C are given by

$$\begin{aligned} &M_{11} = I_1 + I_2 + 2W_2L_1\cos(\theta_e) + W_1L_1^2, \\ &M_{12} = M_{21} = I_2 + W_2L_1\cos(\theta_e), M_{22} = I_2, \\ &C_{11} = -2W_2L_1\sin(\theta_e)\dot{\theta}_s, \\ &C_{12} = -C_{21} = -W_2L_1\sin(\theta_e)\dot{\theta}_s, C_{22} = 0 \end{aligned} \tag{A.2}$$

where θ_e and θ_s are the elbow and shoulder joint angles, L_1 and L_2 are segment lengths, I_1 and I_2 are inertia parameters, and W_1 and W_2 are other parameters.

The controller receives a desired minimum jerk trajectory in joint coordinates as in [19]:

$$\begin{aligned} x(t) &= x_0 + (x_0 - x_f)\left(15\tau^4 - 6\tau^5 - 10\tau^3\right) \\ y(t) &= y_0 + (y_0 - y_f)\left(15\tau^4 - 6\tau^5 - 10\tau^3\right) \end{aligned} \tag{A.3}$$

where $\tau = t/t_f$, x_0, y_0 are the initial hand position coordinates at $t = 0$, and x_f, y_f are the final hand position coordinates at $t = t_f$.

Appendix B

Simulation parameters

In the simulation, fixed weights from desired state to granule cells are initialized by random variables N(0,1), when the modifiable weights of parallel fiber-Purkinje cell synapses are initially set to zero. The simulation has 50 Purkinje cells per each joint that produce feedfoward motor commands for shoulder and elbow independently. The μ-values for the IO neurons are set inhomogeneously as $\mu \in [0.99 \cdot 1.65, 1.01 \cdot 1.65]$. Other simulation parameters are given as Table B.1.

Table B.1: Simulation parameters

Parameter	Value	Unit
η_1	0.04	
η_2	0.04	
I_0	0.05	
β	0.03	
α	0.005	
L_1	0.33	m
L_2	0.34	m
I_1	0.067	$kg \cdot m^2$
I_2	0.97	$kg \cdot m^2$
W_1	1.52	kg
W_2	0.34	$kg \cdot m$
K_P	100	
K_D	1	
dt	0.02	s

Bibliography

[1] Ito M., The cerebellum and neural control, *Raven Press*, 1984.

[2] Purves D., Augustine G. J., Fitzpatrick D., Hall W. C., LaMantia A.S., McNamara J. O., Williams M. S., Neuroscience, *Sinauer Associates, Inc.*, 2004.

[3] Kawato M., Furukawa K., Suzuki R., A hierarchical neural-network model for control and learning of voluntary movement, *Biological Cybernetics*, 57: 169-185, 1987.

[4] Kawato M., Gomi H., A computational model of four regions of the cerebellum based on feedback-error learning, *Biological Cybernetics*, 68: 95-103, 1992.

[5] Marr D., A theory of cerebellar cortex, *The journal of Physiology*, 202: 437-470, 1969.

[6] Albus J. S., The theory of cerebellar function, *Mathematical Biosciences*, 10: 25-61, 1971.

[7] Schweighofer N., Doya K., Fukai H., Chiron J. V., Furukawa T., Kawato M., Chaos may enhance information transmission in the inferior olive, *Proceedings of the National Academy of Sciences of the United States of America*, 101: 4655-4669, 2004.

[8] Tokuda T. I., Han C. E., Aihara K., Kawato M., Schweighofer N., The role of chaotic resonance in cerebellar learning, *Neural Network*, 23: 836-842, 2010.

[9] Uusisaari M., Schutter E. D., The mysterious microcircuitry of the cerebellar nuclei, 2011.

[10] Kawato M., Kuroda S., Schweighofer N., Cerebellar supervised learning revisited: biophysical modeling and degrees-of-freedom control, *Current Opinion in Neurobiology*, 21: 1-10, 2011.

[11] Best A. R., Regehr W. G., Inhibitory regulation of electrically coupled neurons in the inferior olive is mediated by asynchronous release of GABA, *Neuron*, 62: 555-565, 2009.

[12] Gilbert P. F., Thach W. T., Purkinje cell activity during motor learning, *Brain Research*, 128: 309-328, 1977.

[13] Katori Y., Lang E., Onizuka M., Kawato M., Aihara K., Quantitative modeling of spatio-temporal dynamics of inferior olive neurons with a simple conductance-based model, *International Journal of Bifurcation and Chaos*, 3: 585-603, 2010.

[14] Onizuka M., The effect of inhibitory synaptic input on glomeruli in the inferior olive, *NAIST Master thesis*, 2009.

[15] Pikovsky A., Rosenblum M., Kurths J., Synchronization: A universal concept in nonlinear sciences, *Cambridge University Press*, 2001.

[16] Schweighofer N., Arbib M. A., Kawato M., Role of the cerebellum in reaching movements in humans. I. Distributed inverse dynamics control, *European Journal of Neuroscience*, 10: 86-94, 1998.

[17] Strogatz S. H., From Kuramoto to Crawford: exploring the onset of synchronization in populations of coupled oscillators, *Physica D*, 143: 1-20, 2000.

[18] Wolpert D. M., Miall C.R., Katato M., Internal models in the cerebellum, *Trends in Cognitive Sciences*, 2: 338-347, 1998.

[19] Flash T., Hogan. N, The coordination of arm movements: an experimentally confirmed mathematical model, *Journal of Neuroscience*, 5: 1688-1703, 1985.